

**Supplemental Figure S1.** Polarized MTs are essential for cellular localization of axis determinants in the oocyte. A schematic view of the germarium is shown at the top. The oocytes, a germline stem cell (GSC) and cystoblasts (CBs) are shown in purple, pale orange and blue, respectively. A schematic diagram of an ovariole is shown in the middle. The ovariole consists of the germarium at the anterior tip and egg chambers of increasing age. Schematic views of egg chambers at stages 1-8 (mid-oogenesis) are shown at the bottom. MT distribution is shown in green. At stages 1-6, MTs extend along the cortex and fold back slightly at the anterior. The MTOC is detected at the posterior region of the stage 1 oocyte. The oocyte nucleus is encapsulated by MTs. By stage 7, MTs are rolled up in the shape of a “diaphragm” in the center of the oocyte. In stages 8-9, as the ‘diaphragm’ has opened, MT bundles project from both the anterior and the oocyte nucleus in the A-P direction, exhibiting a “horseshoe-like” pattern.

**Supplemental Figure S2.** (A) Mael is expressed in ovaries and *Drosophila* S2 cells, a non-gonadal somatic cell line originally established from an embryo (left panel). Mael can be efficiently knocked down by transfection of double-stranded *mael* RNA in S2 cells (right panel). (B) The Mael signal disappeared from S2 cells after RNAi treatment, confirming that the antibody is Mael-specific. (C) Immunofluorescence analysis of Mael in dividing S2 cells. Mael is highly concentrated at mitotic spindles. (D) The Mael signal was not detected in *mael* mutant (*mael*<sup>M391</sup>/*Df*) egg chambers, confirming the antibody specificity. Scale bars indicate 20  $\mu$ m. (E) Immunoprecipitation was performed from ovary lysates using an anti-Mael monoclonal antibody in an Empigen-based buffer. The immunoprecipitated complexes were stained with silver. Mael alone was immunoprecipitated, confirming that the antibody does not cross-react

with proteins other than Mael. (F) The complexes immunoprecipitated from control (*mael*<sup>M391</sup>/*TM3*) and *mael* mutant (*mael*<sup>M391</sup>/*Df*) ovary lysates using an anti-Mael monoclonal antibody were immunoblotted using antibodies against Cnn, Msps, D-TACC and  $\gamma$ Tub. Mael association with Cnn, Msps, D-TACC and  $\gamma$ Tub was confirmed.

**Supplemental Figure S3.** (A) The Mael complex immunopurified from ovaries with an anti-Mael antibody was analyzed by immunoblotting (IB) with antibodies for each member of the Argonaute family of proteins. The Mael complex does not contain any members of the Argonaute family. (B) Immunoprecipitation from ovary lysates using anti-Aub and anti-Piwi monoclonal antibodies. Protein components of MTOC (Cnn and D-TACC) were not detected in the Aub- and Piwi-associated complexes. (C-D) The Aub- or Piwi-associated complexes purified from ovaries were analyzed by immunoblotting (IB) with the anti-Mael antibody. Mael was not detected in either complex. “n.i.” indicates non-immune IgG used as a negative control.

**Supplemental Figure S4.** Immunohistochemical analyses of the *mael* mutant ovaries using anti-Mael (magenta) and anti-Vas (green) antibodies. Vas is a germ cell marker. Mael was detected both in germline cells and in the Vas-negative somatic follicle cells (surrounded by the dotted-line). Mael was also detected at the mitotic spindles (arrows) in the dividing cyst cells, which are a Vas-positive cyst. DNA was stained with DAPI (blue).

**Supplemental Figure S5.** The expression level of  $\alpha$ Tub in control and *mael*

(*mael*<sup>M391</sup>/*Df*) ovaries. Western blot analyses of ovary lysates using anti-Mael (upper) and anti- $\alpha$ Tub (middle) antibodies. Ponceau S staining of the blot is shown as a loading control (lower).

**Supplemental Figure S6.** Monitoring MT dynamics in living S2 cells using time-lapse fluorescence microscopy. (A) Live fluorescence microscopy cell analysis of *mael*<sup>RNAi</sup> cells showed delayed mitosis. The time that cells take from metaphase to anaphase was measured (also see C). The mitotic time of *mael*<sup>RNAi</sup> cells is longer than that of control cells. (B) The percentage of mitotic S2 cells in *mael*<sup>RNAi</sup>, *cnn*<sup>RNAi</sup>, and *cdc27*<sup>RNAi</sup> S2 cells. *GFP*<sup>RNAi</sup> was used as a control. The number of mitotic cells of *mael*<sup>RNAi</sup> was slightly increased compared to that of *cnn*<sup>RNAi</sup>. *cdc27* is known to be an essential cell cycle gene and was used as a positive control (Goshima et al. 2007) in this study. (C) Time-lapse fluorescence microscopy imaging of control (top) and *mael*<sup>RNAi</sup> (bottom) S2 cells. AcGFP- $\alpha$ Tub and dsRed-Histone 2B were used to detect  $\alpha$ Tub (green) and chromosomes (red), respectively. Normal bipolar spindle formation during cell division appeared normal in *mael*<sup>RNAi</sup> S2 cells. However, *mael*<sup>RNAi</sup> S2 cells showed, in comparison to the control cells, slightly delayed mitosis (also see A). Time scale is in min:sec.

**Supplemental Figure S7.** MT distribution in *mael* egg chambers containing over 16 germ cells visualized using anti- $\alpha$ Tub antibody (white). (A) An egg chamber with two oocyte-like cells was observed in *mael* ovaries. The accumulation of MTs was not detected in either oocyte (green arrowheads). Oo indicates Oocyte-like nuclei. (B) Magnified views (bottom) of *mael* (*mael*<sup>M391</sup>/*Df*) oocytes (indicated with the

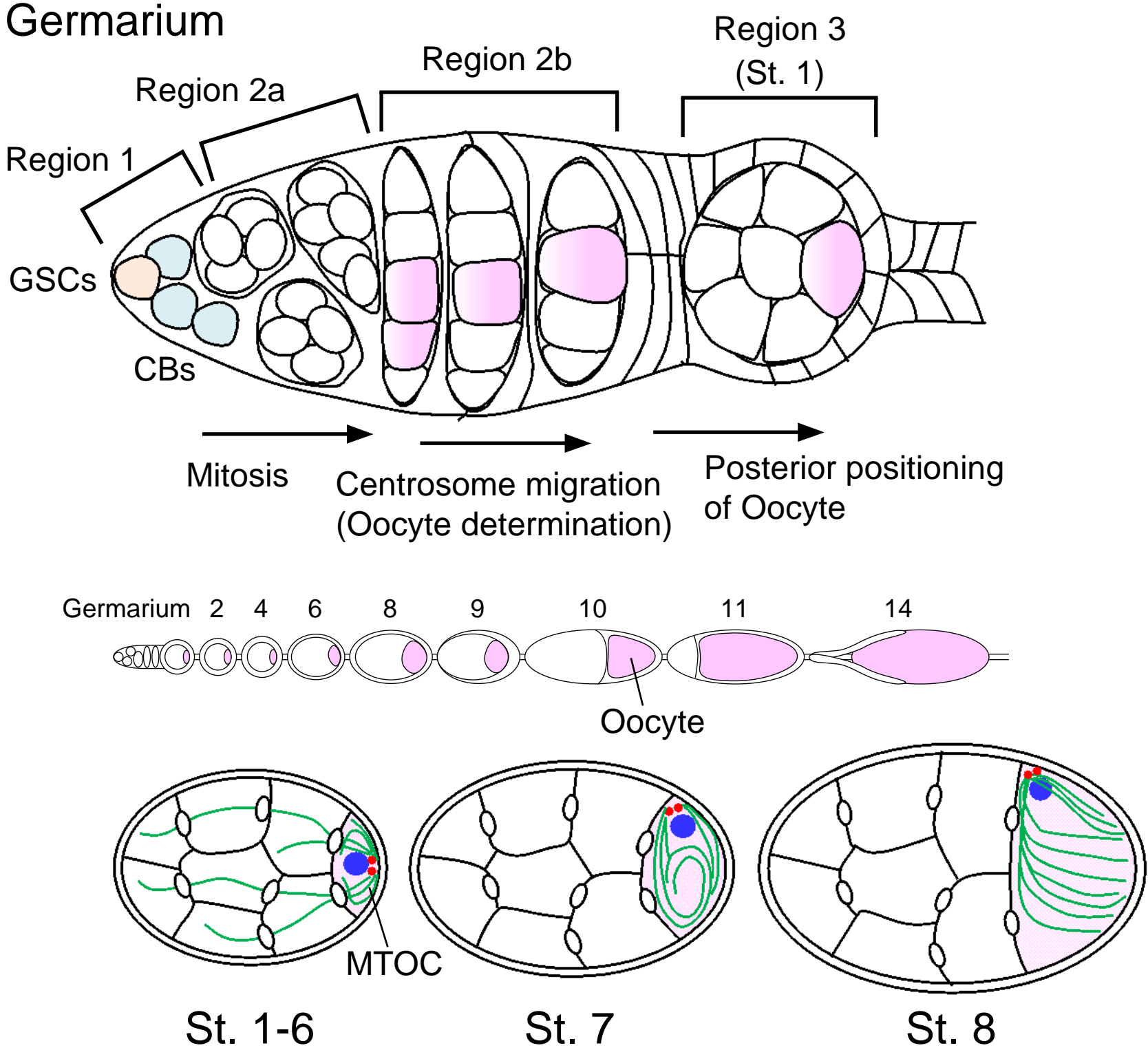
dotted-line) in (A) are shown. Magnified view of control (*mael*<sup>M391</sup>/*TM3* shown in Fig. 5C-St 4-5), which shows MT accumulation at the posterior region of the oocyte, is also shown. It appears that the MTOC is not formed in the *mael* egg chambers. DNA was stained with DAPI (blue).

**Supplemental Figure S8.** Distribution of *DE*-cadherin in *mael* mutant ovaries. (A) The expression pattern of *DE*-cadherin in the germarial region of the control ovary. High concentrations of *DE*-cadherin are found in both anterior and posterior follicle cells (arrows). Oocytes, judged by Orb staining (A'), lie adjacent to *DE*-cadherin-positive follicle cells (A''). (B) The expression pattern of *DE*-cadherin in the germarial region of the *mael* mutant ovary. *DE*-cadherin in both anterior and posterior follicle cells was not detected in *mael* ovaries. *DE*-cadherin was detected in the *mael* oocyte (indicated with an arrow, compare with A). In addition, *DE*-cadherin was localized in a disorderly fashion in some egg chambers (indicated with horizontal square bracket). (C) The expression pattern of *DE*-cadherin in the *mael* mutant egg chamber with over 16 germ cells. *DE*-cadherin accumulated not only in the posterior- but also in the anterior-localized oocyte. DNA was visualized using DAPI. Scale bars indicate 20  $\mu$ m.

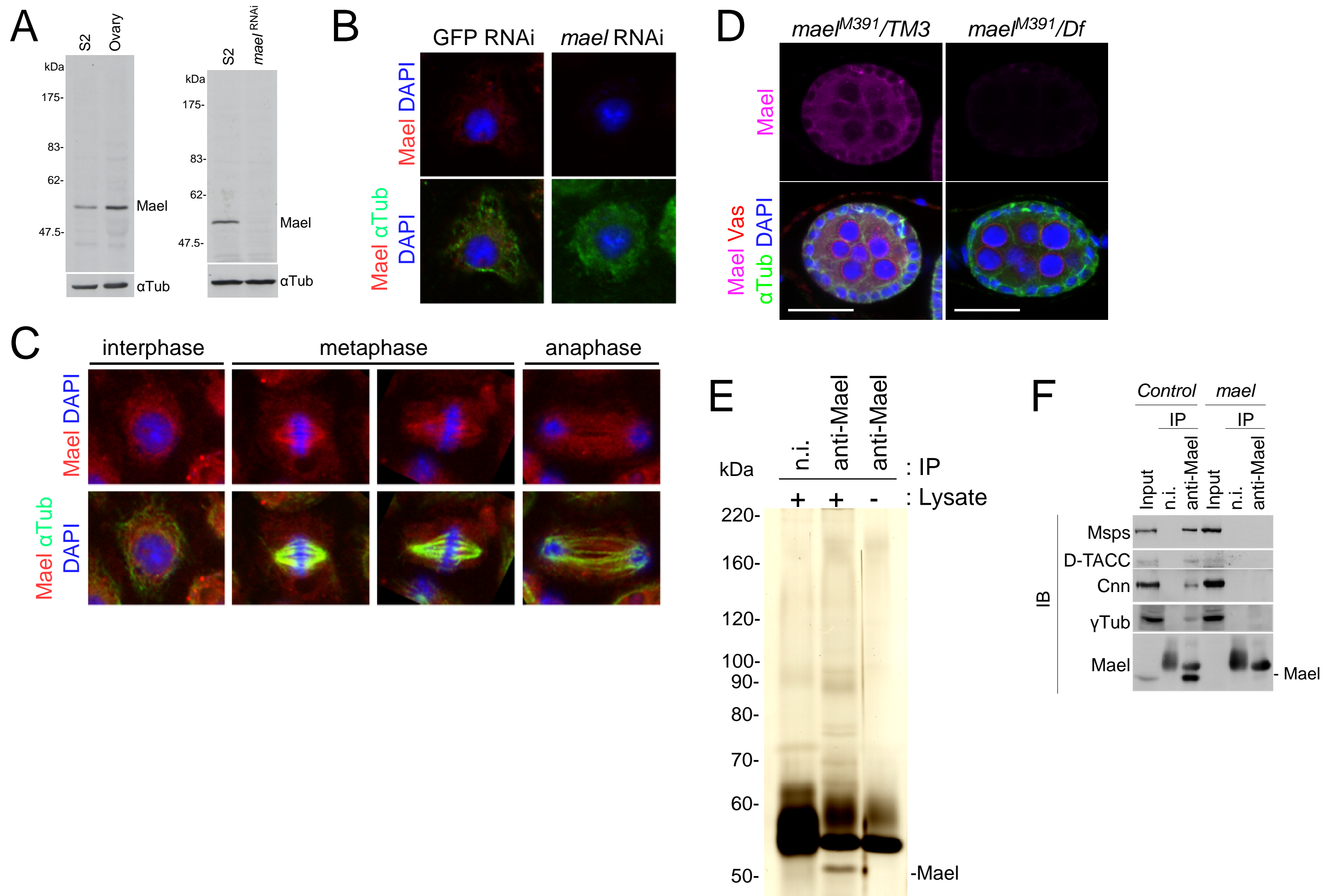
**Supplemental Figure S9.** Possible models for mechanisms giving rise to the egg chambers containing over 16 germ cells, based on Huynh (Huynh 2006). In *Drosophila*, the cystoblast divides precisely four times with incomplete cytokinesis to form a 16-cell cyst. Normal egg chambers contain 15 nurse cells, an oocyte, and 15 ring canals (Normal). When two egg chambers juxtaposed to each other are fused, one egg chamber contains 30 nurse cells, two oocytes and 30 ring canals (Fusion). Cysts with insufficient

rounds of cell division generates less than 15 nurse cells and ring canals (mitotic defects: less than 4 rounds of cell division). A cyst with an extra round of cell division generates 31 nurse cells and ring canals, and an oocyte (mitotic defects: 5 rounds of cell division). In the case of fusion, the number ( $r$ ) of ring canals is  $n-2$ , where  $n$  is the number of germ cells ( $r = n-2$ ), whereas in the case of mitotic defects, the number of ring canals is  $n-1$  ( $r = n-1$ ). White circles indicate germ cells, blue circles indicate oocytes, and red lines indicate ring canals.

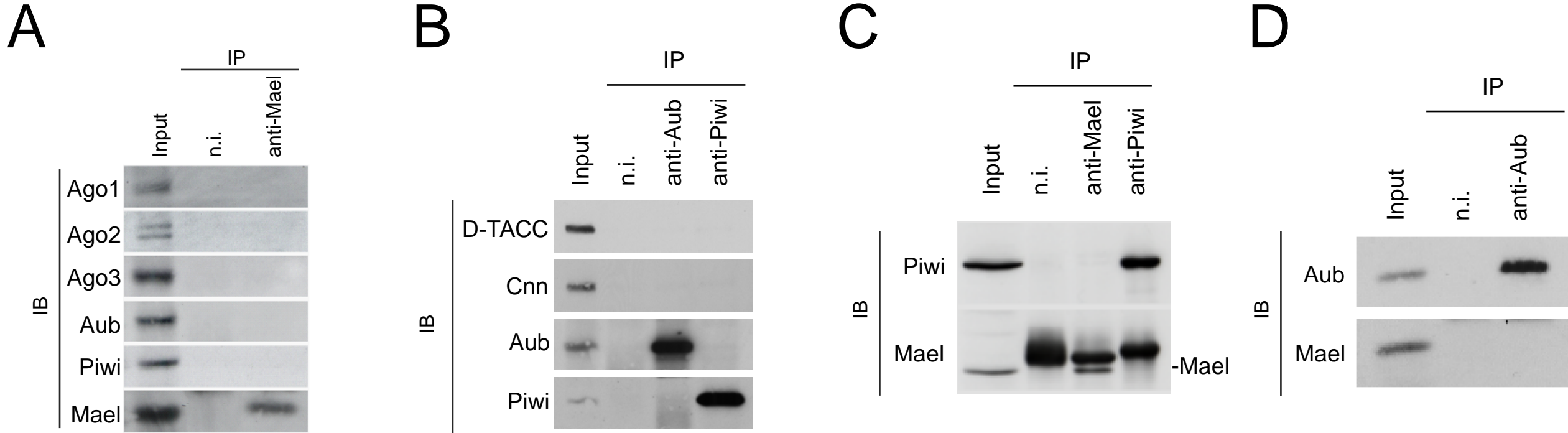
Sato\_supplemental Fig.S1



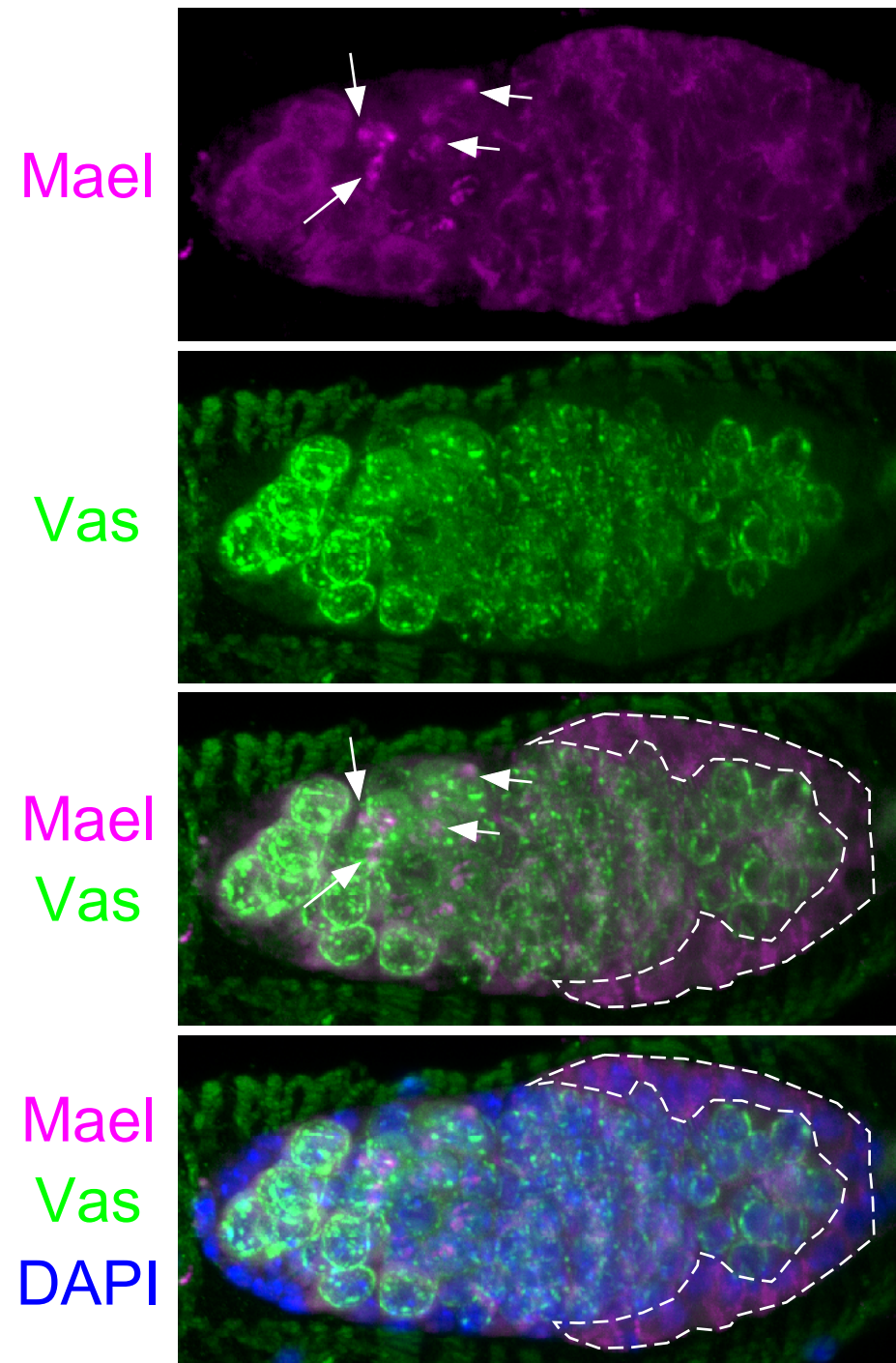
Sato\_supplemental Fig.S2



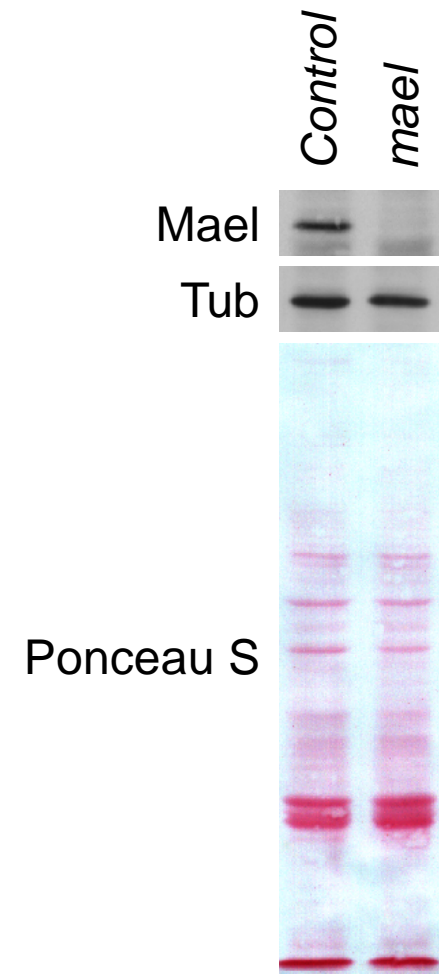
Sato\_supplemental Fig.S3

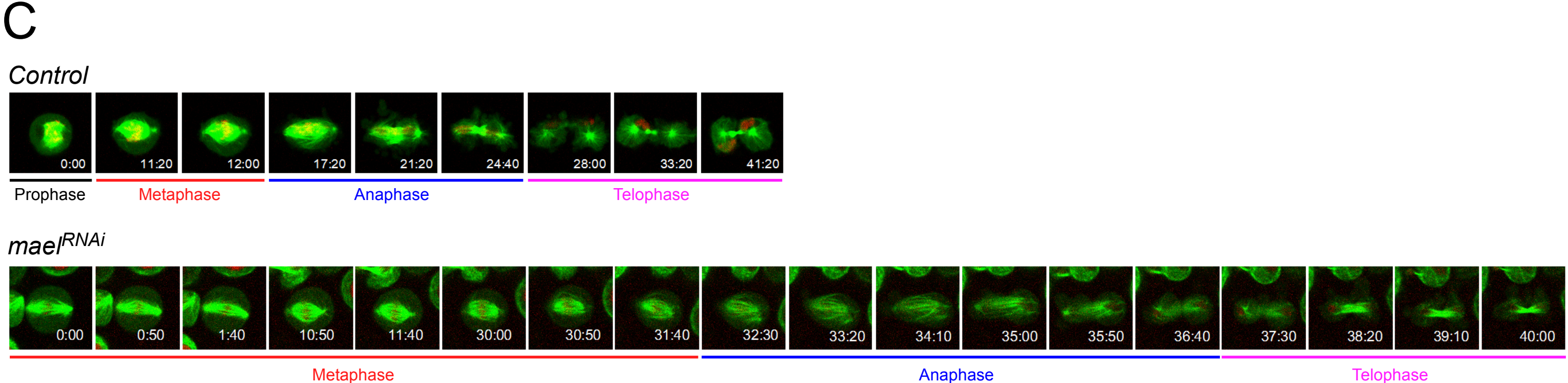
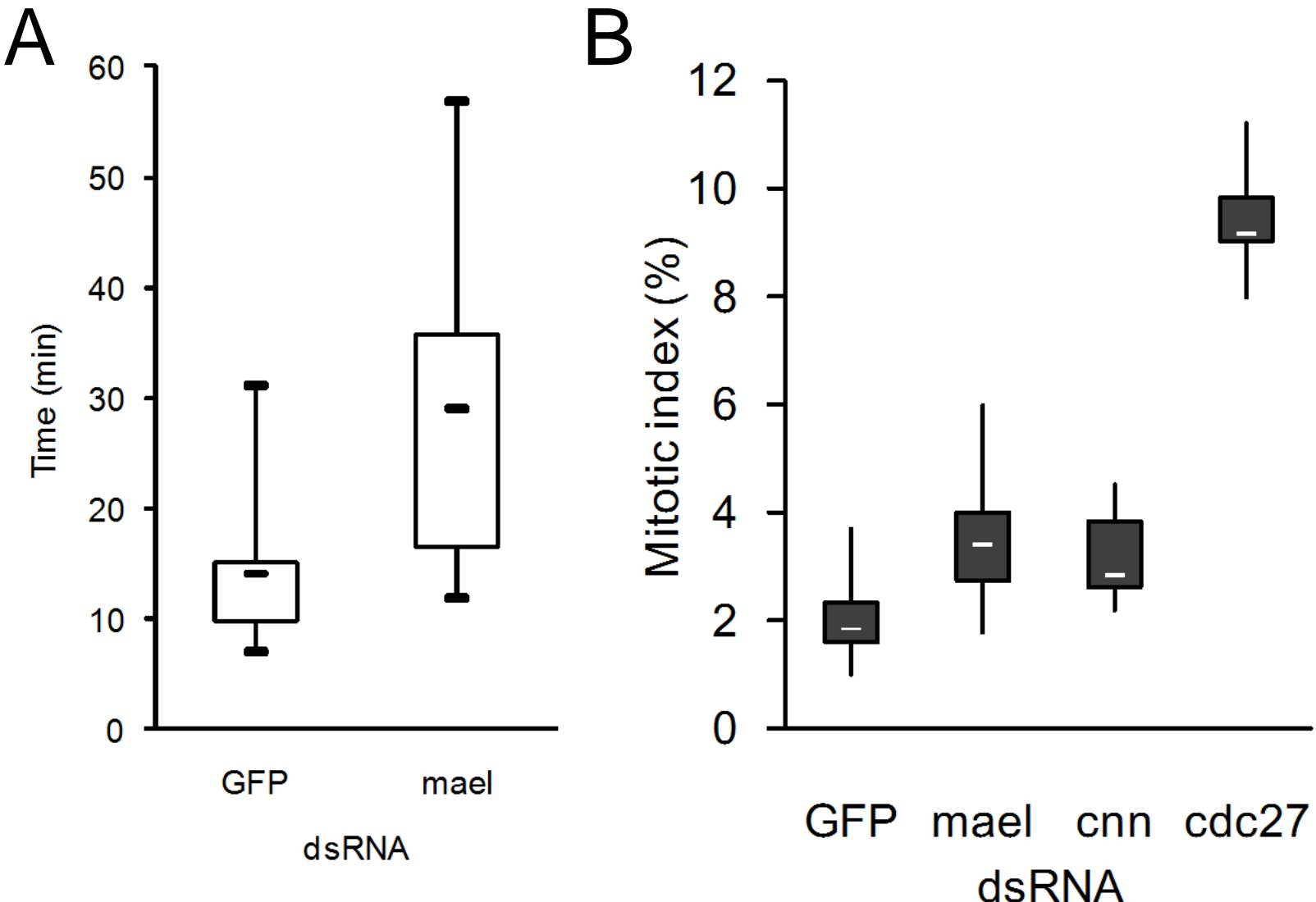


Sato\_supplemental Fig.S4

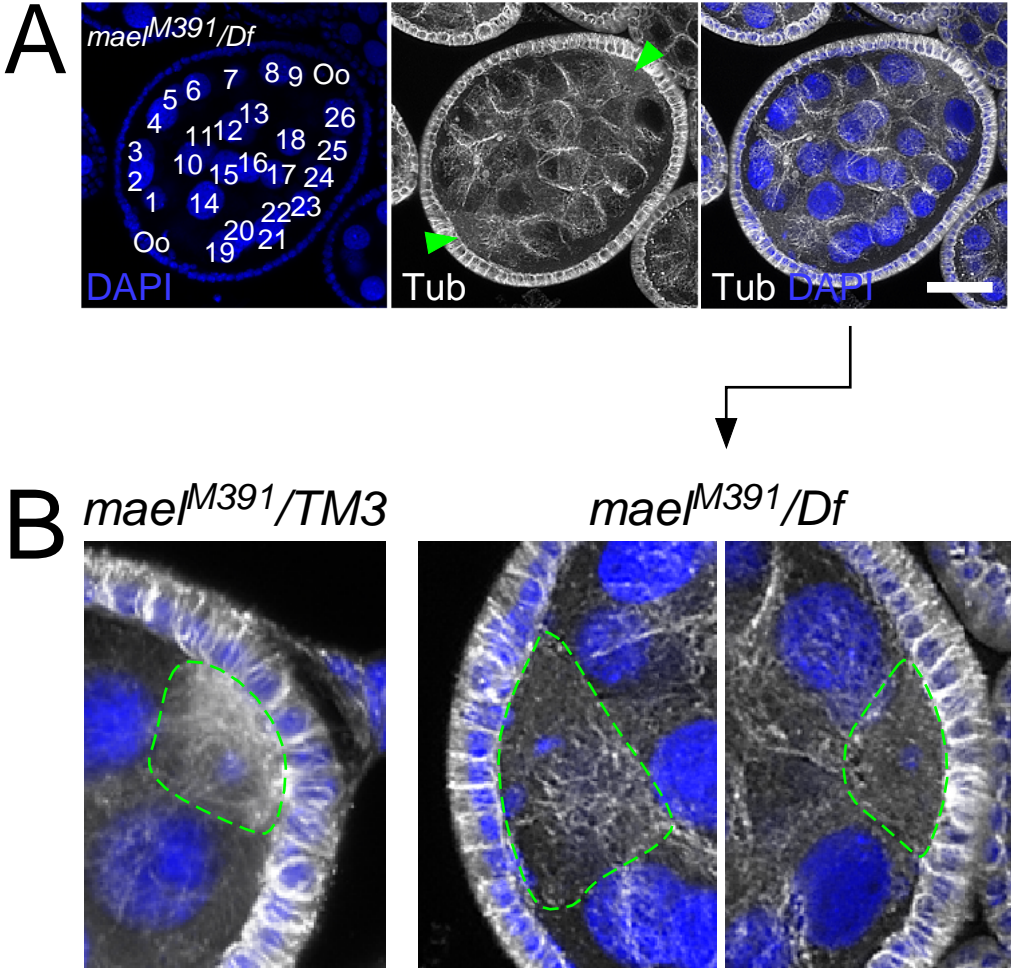


Sato\_supplemental Fig.S5

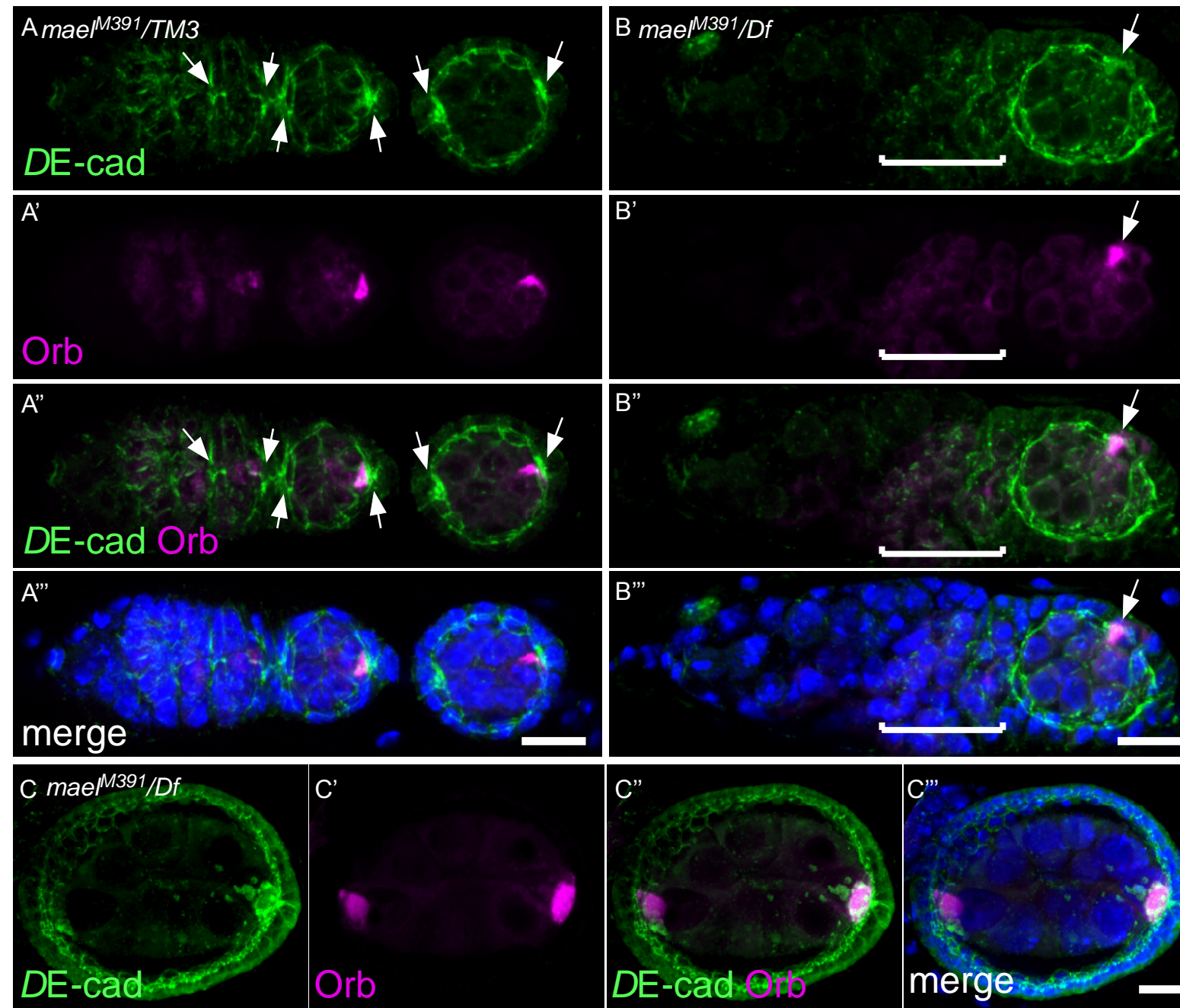




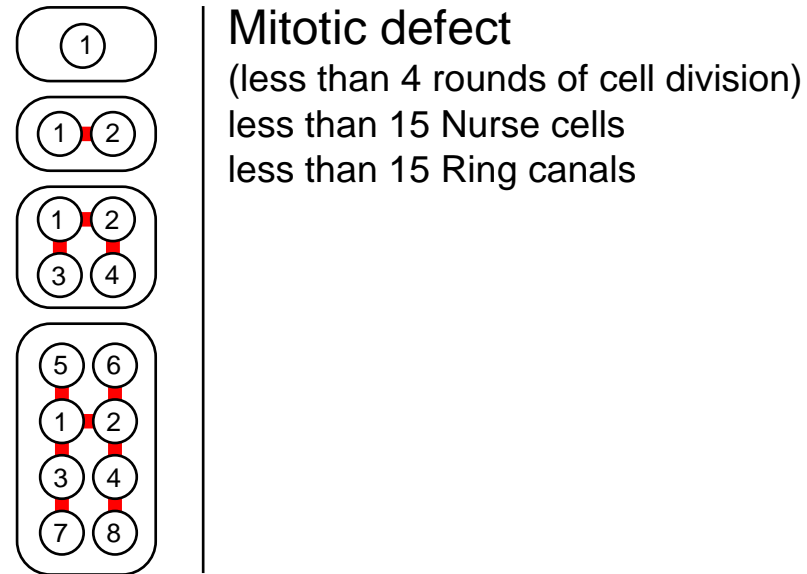
Sato\_supplemental Fig.S7



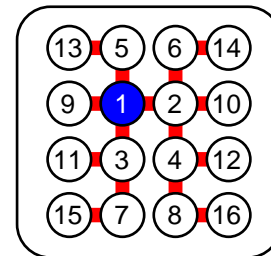
Sato\_supplemental Fig.S8



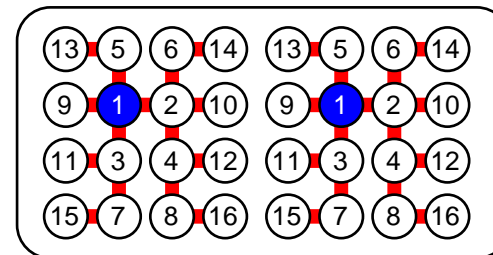
# Sato\_supplemental Fig.S9



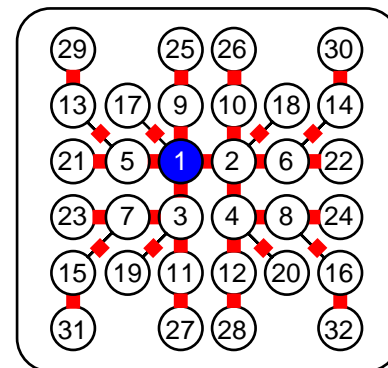
**Mitotic defect**  
 (less than 4 rounds of cell division)  
 less than 15 Nurse cells  
 less than 15 Ring canals



**Normal**  
 (4 rounds of cell division)  
 15 Nurse cells  
 15 Ring canals  
 1 Oocyte



**Fusion**  
 30 Nurse cells  
 30 Ring canals  
 2 Oocyte



**Mitotic defect**  
 (5 rounds of cell division)  
 31 Nurse cells?  
 31 Ring canals  
 1 Oocyte?